

# OLLIE: Derivation-based Tensor Program Optimizer

Liyan Zheng †, Haojie Wang †, Jidong Zhai†, Muyan Hu†, Zixuan Ma†,  
Tuowei Wang†, Shizhi Tang†, Lei Xie†, Kezhao Huang†, Zhihao Jia ‡

†Tsinghua University

‡Carnegie Mellon University

## Abstract

Boosting the runtime performance of deep neural networks (DNNs) is critical due to their wide adoption in real-world tasks. Existing approaches to optimizing the tensor algebra expression of a DNN only consider expressions *representable* by a fixed set of predefined operators, missing possible optimization opportunities between *general* expressions. We propose OLLIE, the first derivation-based tensor program optimizer. OLLIE optimizes tensor programs by leveraging transformations between *general* tensor algebra expressions, enabling a significantly larger expression search space that includes those supported by prior work as special cases. OLLIE uses a *hybrid* derivation-based optimizer that effectively combines explorative and guided derivations to quickly discover highly optimized expressions. Evaluation on seven DNNs shows that OLLIE can outperform existing optimizers by up to  $2.73\times$  ( $1.46\times$  on average) on an A100 GPU and up to  $2.68\times$  ( $1.51\times$ ) on a V100 GPU, respectively.

## 1 Introduction

Fast execution of deep neural networks (DNNs) is critical in a variety of tasks, such as autonomous driving [17, 24, 28], object detection [16, 19], speech recognition [6, 18], and machine translation [37, 39]. A DNN is generally represented as a *tensor program*, which is a directed graph defining the tensor operators (e.g., convolution, matrix multiplication) performed on a set of tensors (i.e.,  $n$ -dimensional arrays).

To optimize the runtime performance of a DNN, many existing frameworks, including TensorFlow, PyTorch, and TensorRT, rely heavily on *manually-designed* rules to map the tensor operators in the DNN to vendor-provided kernel libraries [4, 31, 35]. Although widely used, this rule-based approach requires extensive engineering efforts and only performs optimizations manually discovered.

Recent work has proposed a variety of *automated* approaches that optimize DNN computation by searching over a set of candidate program transformations. We classify existing approaches into two categories based on their search spaces.

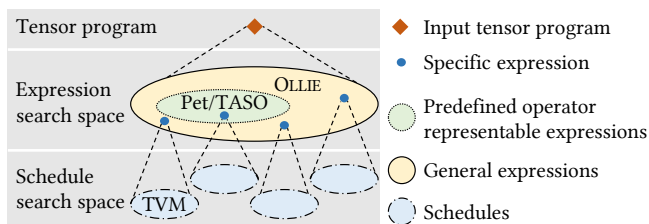


Figure 1: Comparing OLLIE’s search space with those of prior work.

The first category of work explores the *expression* search space. For a given tensor program, a *tensor algebra expression* defines a potential algorithm to compute the program’s output from the input tensors. For example, the computation for a convolution can be expressed as direct convolution, image-to-column, or other algorithms [9, 13]. TASO [21] and PET [38] explore the expression search space using automatically generated transformations between tensor operators. Both of them use a *superoptimization-based* approach that generates expression transformations by enumerating possible combinations of a fixed set of predefined operators. While TASO and PET have demonstrated superior performance over rule-based optimizers, they only discover transformations between expressions that can be constructed using only the predefined operators. These expressions are referred to as *predefined operator representable (POR)* expressions.

The second category of work is motivated by Halide’s idea of compute/schedule separation [33] and optimizes tensor programs by exploring the *schedule* search space. Examples include TVM [10] and Anso [40]. For a given expression, a *schedule* specifies a strategy to execute the computation defined by the expression on a particular hardware device. Although effective at generating high-performance low-level kernels for individual expressions, the schedule-based optimizers only consider schedules that faithfully execute the computation defined by a given expression but miss optimizations that depend on other functionally equivalent expressions.

**Our Approach.** This paper presents OLLIE, the first *derivation-based* tensor program optimizer. OLLIE explores

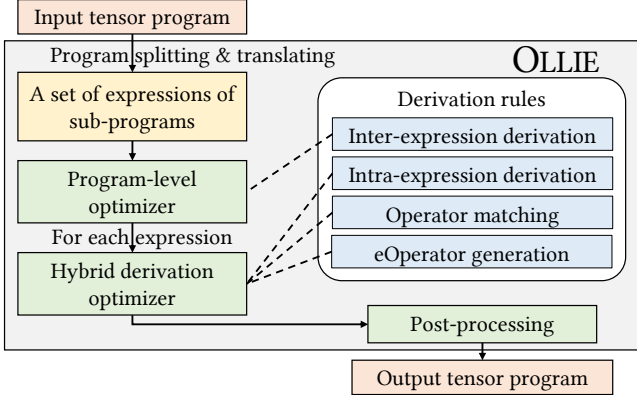


Figure 2: OLLIE overview

the *expression* search space and therefore is orthogonal and can be combined with existing schedule-based optimizers. Figure 1 depicts a comparison between OLLIE’s search space with those of existing automated approaches. A key difference between OLLIE and prior work (i.e., TASO and PET) is that OLLIE is able to explore a significantly larger search space of *general* expressions, which includes the POR expressions supported by TASO and PET as special cases. This generalization unlocks a new class of expression-level optimizations; for example, as we will discuss in §2, OLLIE is able to automatically discover multiple ways to transform a convolution to other (non-POR) expressions, some of which outperform the best convolution algorithms of prior work.

A challenge OLLIE must address is automatically discovering transformation opportunities between *general* expressions. Directly considering general expressions in existing superoptimization-based approach is infeasible, since a superoptimizer discovers transformations by enumerating all possible operators, which can be infinitely many for general expressions. To address this challenge, a key idea behind OLLIE is a *derivation-based* mechanism that automatically transforms a tensor algebra expression to functionally equivalent alternatives by applying a collection of novel derivation rules. Most derived expressions cannot be simply decomposed into predefined operators; thus we introduce *eOperators* to represent the non-POR parts of an expression. eOperators enable OLLIE to generate performance-improving transformations between *general* expressions. For example, as we will discuss in §2 and shown in Figure 3b, OLLIE can optimize a convolution by transforming it to a matrix multiplication (i.e., a predefined operator) and an element-wise addition with customized offsets (an eOperator).

Figure 2 shows an overview of OLLIE. For an input tensor program, OLLIE first splits the program into a number of subprograms by adopting the program splitting mechanism from prior work [38, 40]. Each subprogram is translated to a tensor algebra expression. Second, OLLIE’s *program-level optimizer* applies inter-expression derivation rules to explore optimization opportunities across expressions, such as fusing multiple expressions into one.

A core component of OLLIE is a *hybrid derivation optimizer* that optimizes each subprogram by exploring its expression search space. OLLIE uses a set of intra-expression derivation rules to transform a candidate expression to equivalent alternatives. During the search, OLLIE opportunistically matches a part of the expression with predefined operators using an *operator matching* algorithm, which allows OLLIE to leverage the vendor-provided heavily-optimized kernels (e.g., cuDNN [13] and cuBLAS [14]) to execute the matched part of the expression. OLLIE generates eOperators for the remaining part of the expression.

Optimizing an expression may require applying a long sequence of derivation rules (e.g., our motivating example in §2 uses seven derivation rules), which cannot be efficiently discovered by a fully randomized search algorithm. To address this challenge, OLLIE employs a *hybrid* search approach that performs *explorative* derivations for the initial rounds of the search, allowing OLLIE to explore a comprehensive collection of expressions. For each candidate expression, OLLIE then applies *guided* derivations to derive the expression toward target tensor operators using selected rules. This hybrid approach allows OLLIE to discover complex optimizations, each of which requires a long sequence of derivations, under a reasonable search budget.

Finally, OLLIE selects the best discovered expression for each subprogram and post-processes the expressions to construct an optimized tensor program.

We evaluate OLLIE on seven real-world DNN models that cover a variety of machine learning tasks. We compare OLLIE with state-of-the-art frameworks on two widely used GPU platforms, NVIDIA Tesla A100 and V100. Evaluation shows that OLLIE is up to  $2.73\times$  faster than existing tensor program optimizers. Even for heavily optimized DNNs, such as ResNet-18, OLLIE can still achieve a  $1.33\times$  speedup. The significant performance improvement indicates that OLLIE benefits from the new optimization opportunities enabled by derivation-based expression-level optimizations.

This paper makes the following contributions:

- We extend the expression search space from predefined-operator-representable expressions to general expressions.
- We present the first attempt to explore the significantly larger expression search space using a derivation-based mechanism.
- We build OLLIE, an implementation of the above techniques with over 23K lines of C++ code, which achieves up to  $2.73\times$  speedup over existing tensor program optimizers.

## 2 Motivating Example

As a motivating example, Figure 3a demonstrates the image-to-column optimization [36], which transforms a  $3 \times 3$  convolution (Figure 3a(i)) to a matrix multiplication for devices supporting efficient matrix computations, such as TPUs and GPUs with tensor cores [3, 23]. As shown in Figure 3a(ii), the

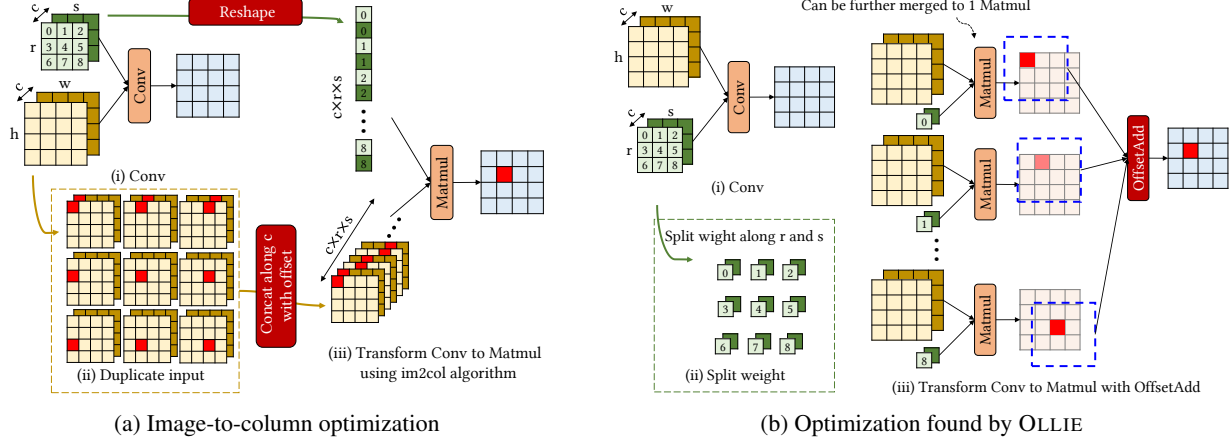


Figure 3: Transform Conv computation to Matmul computation. eOperators are represented as red rounded rectangles. Both figure(i) show a simplified convolution omitting batch dimension and channel dimension of output. It takes an input tensor with size  $(c, h, w)$ , where  $c$ ,  $h$ , and  $w$  represent the input channels, height, and width of images, and a weight tensor with the size of  $(c, r, s)$ , where  $r$  and  $s$  are the height and width of the convolution kernel.

first step of the transformation is duplicating an input image into 9 identical replicas. Second, we concatenate the 9 images into one using different offsets, such that pixels highlighted in red are grouped together in Figure 3a(ii). Finally, we change the layout of the weight (shown in green) to match the dimension of the concatenated image and perform a matrix multiplication, which yields an identical output as the original convolution operator. This optimization has been widely used in different DNN libraries and is implemented by human experts, but OLLIE can find and implement it automatically using expression derivation.

OLLIE is able to find more optimizations. For the same convolution in Figure 3b(i), OLLIE first splits the weight tensor into 9 small weight tensors along  $r$  and  $s$  in Figure 3b(ii). Then, in Figure 3b(iii), each small weight tensor performs matrix multiplication with the input tensor. OLLIE further merges these matrix multiplications into a single one. Finally, the intermediate results are added together to generate an output tensor. Since the addition is taken on each blue dashed region of intermediate tensors, the addition is a customized eOperator `OffsetAdd`, which is automatically generated by OLLIE. This transformation can further improve the performance of evaluated convolution operators by more than two times compared with the cuDNN library on Tesla A100.

However, previous frameworks cannot generate such transformations since: 1) The transformations require eOperators, e.g., adding intermediate tensors with offset, which is outside of the POR expression space explored by superoptimization-based frameworks like TASO and PET. 2) The transformations change the expressions instead of the schedule, and thus cannot be generated by schedule-based optimizers like TVM or Ansor.

$$\begin{aligned}
 & \prod_{c=0}^C \prod_{r=0}^R \sum_{k_0=0}^K \sum_{k_1=0}^K A[c, k_0] B[k_0, k_1] C[k_1, r] \quad (a) \\
 & = \prod_{c=0}^C \prod_{r=0}^R \sum_{k_0=0}^K \left\{ \prod_{c'=0}^C \prod_{k_1=0}^K \sum_{k_2=0}^K A[c', k_1] B[k_1, k_2] \right\} [c, k_0] C[k_0, r] \quad (b)
 \end{aligned}$$

Traversal notation    Summation notation    Scope

Figure 4: Example tensor algebra expressions for two matrix multiplications  $A \times B \times C$ . The red box highlights a scope that instantiates the intermediate result of  $A \times B$ .

### 3 Tensor Algebra Expression

OLLIE represents a tensor program as a *tensor algebra expression* that defines how to compute each element of the output tensor from input tensors. For example, Figure 4 shows the expression for multiplying three matrices. We now explain the components of an expression.

**Traversal and summation notations.** A *traversal notation*, denoted as  $\prod_{x=x_0}^{x_1}$ , consists of an *iterator*  $x$  and an *iterating space*  $[x_0, x_1)$ . The traversal notation corresponds to a dimension of the output tensor, where the iterating space is the range of the dimension. The order between different traversal notations indicates the layout of the output tensor. E.g., in Figure 4,  $\prod_{c=0}^C$  followed by  $\prod_{r=0}^R$  shows that the expression's output is a 2-dimensional tensor with a shape  $C \times R$ .

A *summation notation*, denoted as  $\sum_{x=x_0}^{x_1}$ , corresponds to a dimension with range  $[x_0, x_1)$  that is iterated over when computing each output element. In Figure 4, the summation notation  $\sum_{k_0=0}^K$  indicates that the computation for each output element iterates over an interval with  $K$  elements. Note that OLLIE's expression notation is invariant under permutation of summation notations, which corresponds to different *schedules* of an expression and therefore is not considered in the expression search space.

Tensors are indexed by a *linear combination* of multiple iterators or the division or remainder of iterators (e.g.,  $h\%2$ ).

For simplicity, we may merge multiple iterators into one iterator vector in the paper. Iterator space also can be denoted by an integer set or omitted in expressions. For example,  $\mathbf{L}_{c=0}^C \mathbf{L}_{r=0}^R$  can be represented as  $\mathbf{L}_{cr}$  or  $\mathbf{L}_{\vec{x}}^{\mathbb{X}}$ , where  $\vec{x} = (c, r)$  and  $\mathbb{X} = \mathbb{C} \times \mathbb{R}$  is the iterating space.

**Scope.** For a tensor program with multiple operators (e.g., two consecutive matrix multiplications  $A \times B \times C$ ), a common optimization is to instantiate and reuse intermediate results (e.g., caching the output of  $A \times B$ ), which avoids repetitive computation for these results. OLLIE introduces scopes to represent the instantiation of intermediate results and enable their reuse. Formally, a tensor algebra expression is a *scope*, denoted by a surrounding  $\{\}$ , if the output of the expression is instantiated into a tensor, which allows subsequent computation to refer to its output as a tensor and therefore avoids repeated computation of its output. In Figure 4(b), the expression corresponding to  $A \times B$  becomes a scope, which allows subsequent computation to directly refer to the output of this expression as a tensor.

Most of OLLIE’s derivation rules (described in §4) are based on transformations between scopes, including generating new scopes from existing ones, transforming a scope to another form, and merging multiple scopes into one. Transformations between scopes are essential to OLLIE’s performance optimizations.

**Padding** Tensors may have paddings. For example, convolution may access input tensors at a position outside of  $A$ ’s region. We call these positions the paddings of  $A$ , whose elements are 0 if not specified.

**General format.** We represent arbitrary 1-scope expressions in the following format:

$$\mathbf{L}_{\vec{x}}^{\mathbb{X}} \sum_{\vec{y}}^{\mathbb{Y}} f(\mathbf{T}[\tau(\vec{x}, \vec{y})])$$

where  $\mathbf{T} = \{T_0, T_1, \dots\}$  is a list of input tensors,  $\tau(\vec{x}, \vec{y})$  is the indexing function that computes an element index for  $\mathbf{T}$  using iterators  $\vec{x}$  and  $\vec{y}$ , and  $f$  is the computation taking on the indexed elements of  $\mathbf{T}$ .

## 4 Derivation Rules

To discover highly-optimized expressions for an input tensor program, OLLIE uses *derivation rules* to apply transformations on an input expression. Table 1 summarizes the derivation rules used by OLLIE, which are divided into three categories. The proof of these rules are provided in Appendix.

### 4.1 Inter-Expression Derivation

**Expression splitting** divides an expression into two independent expressions by partitioning the traversal space of the expression  $\mathbb{X}$  into two subspaces  $\mathbb{X}_1$  and  $\mathbb{X}_2$  such that  $\mathbb{X} \subseteq \mathbb{X}_1 \cup \mathbb{X}_2$ . The expression splitting rule is as follows:

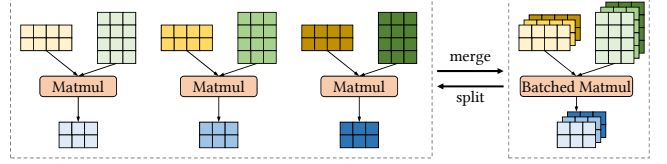


Figure 5: Splitting and merging matrix multiplications.

$$\mathbf{L}_{\vec{x}}^{\mathbb{X}} f(\mathbf{T}[\tau(\vec{x})]) \implies \mathbf{L}_{\vec{x}}^{\mathbb{X}_1} f(\mathbf{T}[\tau(\vec{x})]) \sim \mathbf{L}_{\vec{x}}^{\mathbb{X}_2} f(\mathbf{T}[\tau(\vec{x})])$$

where  $\sim$  denotes the independence of the two expressions.

**Expression merging** combines two independent expressions that have identical computation into a single expression by merging the traversal spaces of the original expressions:

$$\mathbf{L}_{\vec{x}}^{\mathbb{X}_1} f(\mathbf{T}[\tau(\vec{x})]) \sim \mathbf{L}_{\vec{x}}^{\mathbb{X}_2} f(\mathbf{T}[\tau(\vec{x})]) \implies \mathbf{L}_{\vec{x}}^{\mathbb{X}} f(\mathbf{T}[\tau(\vec{x})])$$

where  $\mathbb{X}_1 \cup \mathbb{X}_2 \subseteq \mathbb{X}$ . Expression merging is the symmetric transformation of expression splitting.

A typical example of expression splitting and merging is the transformation between `Matmul` and `BatchMatmul`: multiple matrix multiplications can be merged together to a single batch matrix multiplication, and a batch matrix multiplication can be split into multiple matrix multiplications, as shown in Figure 5.

**Expression fusion** fuses multiple dependent expressions into one using the chain rule:

$$\mathbf{L}_{\vec{y}}^{\mathbb{Y}} g(\mathbf{T}'[\pi(\vec{y})]) \circ \mathbf{L}_{\vec{x}}^{\mathbb{X}} f(\mathbf{T}[\tau(\vec{x})]) \implies \mathbf{L}_{\vec{y}}^{\mathbb{Y}} g(\{\mathbf{L}_{\vec{x}}^{\mathbb{X}} f(\mathbf{T}[\tau(\vec{x})])\}[\pi(\vec{y})])$$

where  $\mathcal{E}_1 \circ \mathcal{E}_2$  denotes that the result of expression  $\mathcal{E}_2$  is fed as inputs to expression  $\mathcal{E}_1$  (i.e.,  $\mathbf{T}'$  equals to the computation result of  $\mathbf{L}_{\vec{x}}^{\mathbb{X}} f(\mathbf{T}[\tau(\vec{x})])$ ).

Expression fusion allows OLLIE to consider *operator fusion*, a technique that fuses the computation of multiple operators into a single kernel to reduce data movement and kernel launch overhead.

### 4.2 Intra-Expression Derivation

Intra-expression derivation rules transform an expression into other functionally equivalent forms, which is essential for constructing a comprehensive search space of expressions for a tensor program. Figure 6 shows the intra-expression derivation rules used to discover the optimization in Figure 3b. We now describe these intra-expression derivation rules.

**Summation splitting** divides a summation  $\sum_{\vec{s}}$  in an expression into two summations  $\sum_{\vec{s}_1}$  and  $\sum_{\vec{s}_2}$  and instantiates the result of the inner summation by converting it to a scope:

$$\mathbf{L}_{\vec{x}} \sum_{\vec{s}_1, \vec{s}_2} f(\mathbf{T}[\tau(\vec{x}, \vec{s}_1, \vec{s}_2)]) \implies \mathbf{L}_{\vec{x}} \sum_{\vec{s}_1} \{ \mathbf{L}_{\vec{s}_2} f(\mathbf{T}[\tau(\vec{x}, \vec{s}_1, \vec{s}_2)]) \} [\vec{x}, \vec{s}_1]$$

where  $\tau$  is a mapping from  $(\vec{x}, \vec{s}_1, \vec{s}_2)$  to an input position. OLLIE divides the iterators of a summation into two disjoint groups,  $\vec{s}_1$  and  $\vec{s}_2$ , which splits the summation into two nested scopes  $\mathcal{S}_1, \mathcal{S}_2$ , where  $\mathcal{S}_1 = \mathbf{L}_{\vec{x}} \sum_{\vec{s}_2} f(\mathbf{T}[\tau(\vec{x}, \vec{s}_1, \vec{s}_2)])$  and  $\mathcal{S}_2 = \mathbf{L}_{\vec{x}} \sum_{\vec{s}_1} \mathcal{S}_1[\vec{x}, \vec{s}_1]$ . Note that in summation splitting,

Table 1: Derivation rules for tensor algebra expressions

	Rules	Descriptions
Inter-expression derivation	Expression splitting	Split an expression into multiple independent expressions
	Expression merging	Merge multiple independent expressions into one
	Expression fusion	Fusing multiple dependent expressions into one
Intra-expression derivation	Summation splitting	Split summation from one scopes into two
	Variable substitution	Replace iterators of traversal notations with new ones
	Traversal merging	Merge two scopes into one by merging traversals
	Boundary relaxing	Relax the range of iterators
	Boundary tightening	Tighten the range of iterators
Expression instantiation	Operator matching	Match a scope with operators and replace it by a tensor
	eOperator generation	Generate an eOperator for a scope and replace it by a tensor

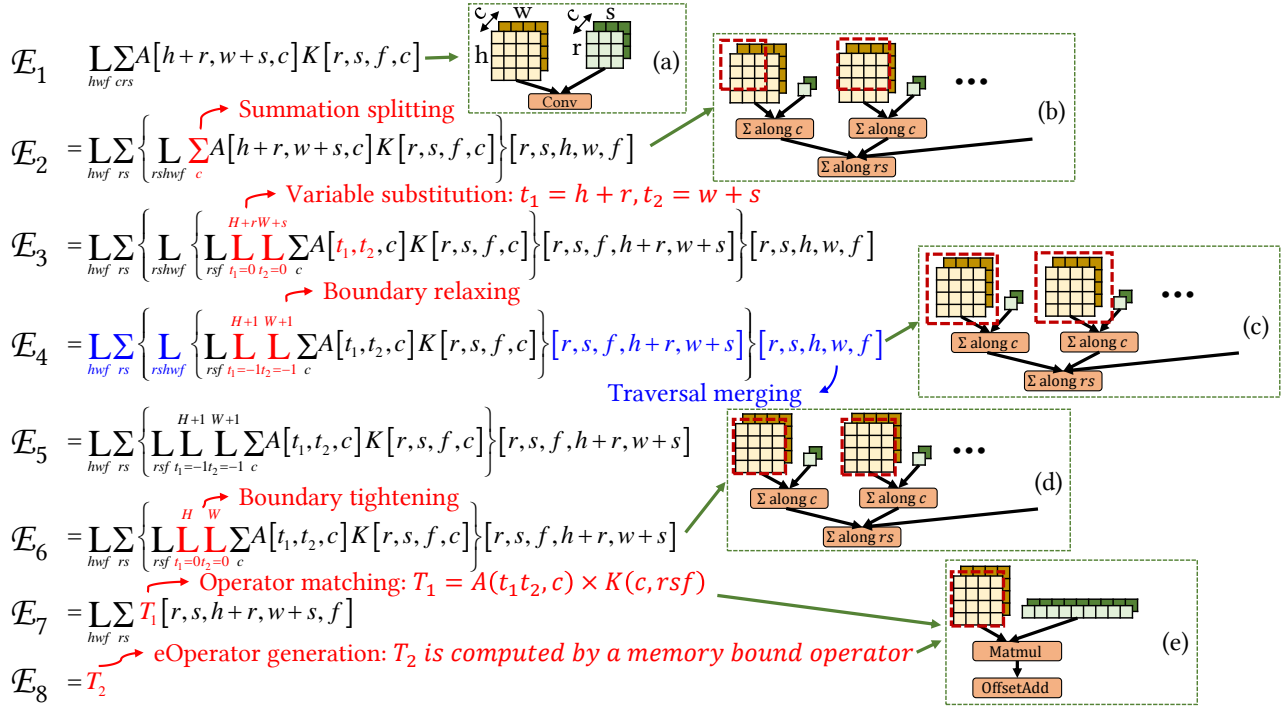


Figure 6: The derivation process of the example in Figure 3b, which replaces Conv with Matmul and eOperators

OLLIE converts the result of the inner summation into a scope, whose output is reused by the outer summation.

To transform a  $3 \times 3$  convolution to a batch of nine matrix multiplications, as shown in Figure 6, OLLIE first transforms the initial expression  $\mathcal{E}_1$  to  $\mathcal{E}_2$  by splitting the summation  $\Sigma_{c r s}$  into two operations  $\Sigma_{r s}$  and  $\Sigma_c$ , and instantiating the output of the inner summation (i.e.,  $\{\mathbb{L}_{r s h w f} \Sigma_c A[h+r, w+s, c] K[r, s, f, c]\}$ ). The inner scope only sums along the  $c$  dimension; as a result, an intermediate 5-dimensional tensor is instantiated since the summation along the  $r$  and  $s$  dimensions is not performed but converted to traversal notations. The outer scope computes the remaining summation over the  $r$  and  $s$  dimensions, which produces a 4-dimensional tensor. Figure 6 (a) and (b) depict the computation graphs before and after this derivation.

**Variable substitution** substitutes a set of traversal iterators  $\mathbb{L}_{\vec{x}}$  with a new set of iterators  $\mathbb{L}_{\vec{y}}$  by applying a *bijective*

function  $\Phi$  (i.e.,  $\vec{y} = \Phi(\vec{x})$ ).<sup>1</sup> This transformation allows the expression to be computed using a different set of traversal iterators. In particular, for an expression  $\mathbb{L}_{\vec{x}} f(\mathbf{T}[\tau(\vec{x})])$ , variable substitution introduces an intermediate scope that computes  $\mathbb{L}_{\vec{y}} f(\mathbf{T}[\tau(\Phi^{-1}(\vec{y}))])$ , where  $\Phi$  is a bijective function that maps  $\mathbb{X}$  to  $\mathbb{Y} = \Phi(\mathbb{X})$ , and  $\Phi^{-1}$  is the reverse function of  $\Phi$ . Formally,

$$\mathbb{L}_{\vec{x}} f(\mathbf{T}[\tau(\vec{x})]) \Rightarrow \mathbb{L}_{\vec{x}} \left\{ \mathbb{L}_{\vec{y}} f(\mathbf{T}[\tau(\Phi^{-1}(\vec{y}))]) \right\} [\Phi(\vec{x})]$$

Variable substitution constructs an intermediate scope with new traversal iterators. To preserve functional equivalence, the original iterator  $\vec{x}$  is used to construct the final result using the output of the intermediate scope.

<sup>1</sup>A mapping function  $\Phi$  is *bijective* if it is both injective (one-to-one) and surjective (onto).

In Figure 6, OLLIE applies variable substitution to transform the expression from  $\mathcal{E}_2$  to  $\mathcal{E}_3$ , using bijective function:  $\Phi(r, s, h, w, f) = (r, s, f, h + r, w + s)$ . Specifically,  $h + r$  and  $w + s$  are substituted with  $t_1$  and  $t_2$  in  $\mathcal{E}_3$ . Note that variable substitution does not change the computation graph.

**Traversal merging** merges the traversal notations in two scopes into a single scope using a bijective function  $\Phi$ :

$$\prod_{\vec{x}} \sum_{\vec{y}} \prod_{\vec{z}} \{ \mathbf{L} f(\mathbf{T}[\tau(\vec{z})]) \} [\Phi(\vec{x}, \vec{y})] \Rightarrow \prod_{\vec{x}} \sum_{\vec{y}} f(\mathbf{T}[\tau(\Phi(\vec{x}, \vec{y}))])$$

where  $\Phi(\mathbb{X} \times \mathbb{Y}) \subseteq \mathbb{Z}$ .

For the example in Figure 6, OLLIE applies traversal merging to transform  $\mathcal{E}_4$  to  $\mathcal{E}_5$ . For this transformation, the outer traversal and summation notations and the inner traversal notation both include five iterators (i.e.,  $\vec{x} = (h, w, f)$ ,  $\vec{y} = (r, w)$ , and  $\vec{z} = (r, s, h, w, f)$ ). Traversal merging is applied with an identity mapping function  $\Phi$  and an indexing function  $\tau(r, s, h, w, f) = (r, s, f, h + r, w + s)$ . Traversal merging removes a scope while preserving the computation graph.

**Boundary relaxing and tightening** inspect whether the computation for some output elements can be avoided if these elements are constants for arbitrary inputs. OLLIE executes constant propagation on expressions to deal with constant numbers in expressions and padding in tensors. If a region of output has constant value, OLLIE converts it into an attribute of tensors to reduce meaningless computation. The following formula shows how boundary relaxing and tightening are performed:

$$\prod_{\vec{x}} f(\mathbf{T}[\tau(\vec{x})]) \iff \prod_{\vec{x}'} f(\mathbf{T}[\tau(\vec{x})])$$

, where  $\mathbb{X} \subset \mathbb{X}'$ , and computation on  $\mathbb{X}' - \mathbb{X}$  will not be used as the results of the tensor program.

In the running example in Figure 6, the formula in  $\mathcal{E}_4$  performs boundary relaxing on  $t_1$  and  $t_2$ , transforming their ranges from  $[0, H + r)$  and  $[0, W + s)$  to  $[-1, H + 1)$  and  $[-1, W + 1)$ , respectively, as  $r$  and  $s$  are in range of  $[-1, 1]$ . After boundary relaxing, the computation graph is transformed from Figure 6 (b) to (c). The formula in  $\mathcal{E}_6$  performs boundary tightening on  $t_1$  and  $t_2$ , transforming their ranges from  $[-1, H + 1)$  and  $[-1, W + 1)$  to  $[0, H)$  and  $[0, W)$ , respectively, as the computation taken on  $t_1 = -1$ ,  $t_1 = H + 1$ ,  $t_2 = -1$  and  $t_2 = W + 1$  will not be used for the output tensor. After boundary tightening, the computation graph is transformed from Figure 6 (c) to (d).

### 4.3 Expression Instantiation

Expression instantiation rules lower expressions into executable kernels. After applying these rules, the instantiated scope is replaced with a tensor in the original expression and separated from the following derivation. OLLIE supports two classes of instantiation, operator matching and eOperator generation, to leverage existing highly optimized kernels and flexibly generate other kernels. In this subsection, we will introduce how these two instantiation rules work.

Table 2: Iterator mapping table

Tensors			Ops			
input	weight	output	Add	Matmul	Conv	G2BMM
✓	✓	✓	$mn$	$b$		$bm$
✓		✓		$m$	$nhw$	
	✓	✓		$n$	$f$	$w$
✓	✓			$k$	$crs$	$k$

#### 4.3.1 Pattern Matching

Mapping a tensor algebra expression to an operator is challenging since an operator can be represented in various expressions with potentially different tensor layouts, tensor shapes, and iterators. For example, the standard tensor algebra expression of a batched matrix multiplication is shown in Expression (1). However, although Expression (2) is significantly different from Expression (1), it can also be directly instantiated as a batched matrix multiplication in math libraries<sup>2</sup>. Similar problems exist for other operators.

$$\prod_{bmn} \sum_k A[b, m, k] B[b, k, n] \quad (1)$$

$$\prod_{bmn} \sum_k C[b, 0, m, 1 + k] D[b - 1, b, k, n] \quad (2)$$

To match a tensor algebra expression to operators, OLLIE uses *iterator mapping table* to summarize linear algebra properties of expressions. Iterator mapping table supports all operators expressible in tensor algebra expression. Table 2 shows typical operators, including an element-wise operator, matrix multiplication, convolution, and G2BMM [25] (general to band matrix multiplication). The right part of the table list all iterators of an operator, which are categorized into four groups based on whether the iterators appears in the input, weight, and output tensor. Iterator mapping table also records the coefficient of iterators in the index of each tensors for operator matching.

Taking the batched matrix multiplication in Expression (1) as an example, the iterators  $b$ ,  $m$ ,  $n$ , and  $k$  appear in different combinations of the input, weight, and output tensors. These variables are assigned to different *iterator groups*, as shown in Table 2. To match an expression with a specific operator, we need to match the iterators in this expression to the iterators in the iterator mapping table.

The detailed matching process is listed as follows:

- Fill iterators into iterator mapping table:** enumerate all the iterators in a given expression, and fill them in into the iterator groups in the iterator mapping table according to which tensor it appears in.
- Match iterator groups:** for each iterator group in iterator mapping table, the number of iterators should be the same.
- Match iterators:** if there are multiple iterators in an iterator group, enumerate all one-to-one mapping between variables of the operator and those of the expression. After the variables are mapped, check whether the coefficients

<sup>2</sup>Math libraries including BLAS allow for specifying the stride of dimensions to work with different input layouts.

of iterators in index match (whether the coefficient of each variable and the correlation between different variables in the expression are consistent with patterns, e.g.,  $h$  and  $r$  should have the same coefficient in the index of input tensor of convolution in Expression  $\mathcal{E}_1$  in Figure 6).

For the example in Equation (2), it has the same iterator groups with `Matmul`. There is an unique one-to-one iterator mapping between the expression and `Matmul` and it matches all iterators. After the pattern match rule succeeds, OLLIE replaces the matched scope with a tensor and generates a corresponding `Matmul` operator in the computation graph.

### 4.3.2 eOperator Generation

For expressions which cannot match existing operators, OLLIE converts them into eOperators and generates executable kernels based on their tensor algebra expressions. Since tensor algebra expressions exactly define the computation semantics, OLLIE is able to feed them into existing code generation frameworks, such as TVM, Halide, and Tiramisu [7]. For example, for the expression in  $\mathcal{E}_7$  of Figure 6, OLLIE lowers it to TVM by converting its iterator space of traversal notation into a tensor and the computation expression into a lambda function. Figure 7 shows the result which can be processed by TVM to automatically generate kernel.

```
T1 = te.placeholder((M, K), name="T1")
r = te.reduce_axis((-1, 2), "r")
s = te.reduce_axis((-1, 2), "s")
T2 = te.compute((H, W, F),
    lambda h, w, f: te.sum(
        # Processing of padding is omitted for conciseness
        T1[r, s, h+r, w+s, f], axis=[r, s]),
    name="T2")
```

Figure 7: Lowering  $\mathcal{E}_7$  in Figure 6 to TVM.

### 4.3.3 Discussion

Although OLLIE can treat arbitrary expressions as eOperators to support various optimizations, the code generation process introduces too much overhead making such optimizations impractical. Considering existing DNN libraries already provide many predefined operators which can outperform generated kernels in most cases, OLLIE adopts the strategy that mapping the expression to the combination of compute-bound predefined operators and memory-bound eOperators. In this way, OLLIE can benefit from both the efficiency of existing libraries and the flexibility of auto-generated eOperators. Moreover, tuning memory-bound operators is much easier than tuning compute-bound ones since the former ones often have much easier schedules. This guarantees OLLIE can find optimized transformations within a promising time. Typically, OLLIE spends around one minutes to generate a memory-bound eOperators.

---

### Algorithm 1 Program-level optimizer.

---

- 1: **Input:** An input tensor program  $\mathcal{P}$
  - 2: **Output:** An optimized tensor program  $\mathcal{P}_{\text{opt}}$
  - 3:
  - 4:  $I\mathcal{R}$  = inter-expression rule set
  - 5:  $\mathcal{SP}$  = split  $\mathcal{P}$  and translate subprograms into expressions
  - 6:  $\mathcal{P}_{\text{opt}} = \emptyset$
  - 7: **for**  $E \in \mathcal{SP}$  **do**
  - 8:     **for**  $r \in I\mathcal{R}$  **do**
  - 9:          $\mathcal{E}' = \text{apply } r \text{ to } E$
  - 10:          $\mathcal{SP} = \mathcal{SP} + \mathcal{E}'$
  - 11: **for**  $E \in \mathcal{SP}$  **do**
  - 12:      $\text{candidates} = \text{HYBRIDDERIVATION}(E)$
  - 13:      $\text{best} = \text{candidate with best performance in } \text{candidates}$
  - 14:     add  $\text{best}$  into  $\mathcal{P}_{\text{opt}}$
  - 15:  $\text{POSTOPTIMIZATION}(\mathcal{P}_{\text{opt}})$
  - 16: **return**  $\mathcal{P}_{\text{opt}}$
- 

## 5 Derivation-Based Program Optimizations

In this section, we describe how OLLIE performs derivation-based transformations to optimize tensor programs in §5.1 and §5.2, and related optimization techniques in other subsections.

### 5.1 Program-level optimizer

Algorithm 1 shows the workflow of the program-level optimizer. For an input tensor program, OLLIE first splits it into subprograms using non-linear activation operators as the splitting points. This is because activation operators often do not provide further optimization opportunities other than fusion, as discovered by prior work [38]. For each subprogram, OLLIE translates it into expressions using the predefined expression for each operator. Note that a subprogram may contain several operators and thus includes multiple expressions. For the expressions of each subprogram, OLLIE applies the inter-expressions rules to perform *inter-operator* transformations (Line 9) and then feeds each expression to OLLIE’s hybrid derivation optimizer (see §5.2) for generating *intra-operator* transformations (Line 12). At last, OLLIE merges the transformation with the best performance of each subprogram, performs post-optimizations like fusing the adjacent memory-bound operators, and finally generates an optimized tensor program.

### 5.2 Hybrid Derivation Optimizer

To explore the vast expression transformation space effectively, OLLIE leverages a *hybrid derivation algorithm* to efficiently discover possible transformations. Figure 8 illustrates the procedure of this hybrid derivation algorithm, which includes an explorative derivation stage and a guided

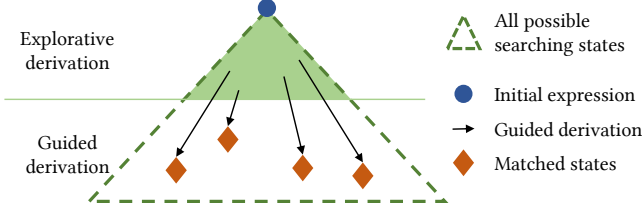


Figure 8: Hybrid derivation algorithm.

derivation stage. During the explorative derivation, OLLIE iteratively applies all derivation rules to current expressions. However, due to the enormous searching states, only adopting explorative derivation will introduce unacceptable searching overhead. To reduce searching overhead, OLLIE adopts guided derivation to match expressions towards target states with the help of iterator mapping table. As mentioned in §4.3.1, the target states are well optimized operators provided by existing kernel libraries, and OLLIE can automatically generate corresponding eOperators inferred by guided derivation to bridge the gap between current searching state and target searching state. Algorithm 2 shows the detailed algorithm of hybrid derivation.

**Explorative derivation** During the explorative derivation, OLLIE tries to apply the derivation rules on the input expression for certain rounds (called *depth*), to explore different functionally-equivalent expressions. The search is controlled by a hyperparameter *MaxDepth*, which determines the maximum depth of derivation steps during explorative derivation (Line 14). To eliminate redundancy, OLLIE generates a fingerprint (§5.3) for each discovered expression. If there is a fingerprint conflict, OLLIE prunes this expression to avoid deriving duplicate expressions (Line 16).

**Guided derivation** OLLIE leverages the guided derivation to derive expressions toward well-optimized operators provided by vendor or other libraries. For each state in explorative derivation, OLLIE selects well-optimized operators  $\mathcal{T}$  as target for guided derivation. When the expression is derived to a single tensor (Line 29), all computation in the expression are replaced with operators or eOperators, which means an equivalent tensor program is discovered for the input expression. OLLIE adds the derived computation graph to the output set. Otherwise, OLLIE continues to leverage guided derivation to derive the current expressions toward the pattern of target operators (Line 32).

OLLIE decides derivation rules by analyzing iterator mapping table mismatches between current expressions and target operators. For the iterator group mismatch, which means more or less iterators exist in a iterator group, OLLIE merges or splits iterators by applying the variable substitution rule on them. While for the iterator mismatches, OLLIE transforms data layouts to satisfy requirements of target operators. Since data layout transformations are achieved by variable substitution on tensor algebra expressions, OLLIE constructs the iterator mapping function  $\Phi$  by looking up

---

**Algorithm 2** Hybrid derivation algorithm.

---

```

1: Input: An input expression  $\mathcal{E}_0$ 
2: Output: A set of tensor program transformations  $\mathcal{P}$ 
3:
4:  $\mathcal{R}$  = intra-expression and instantiation rules set
5:  $\mathcal{O}$  = well-optimized operators
6:  $\mathcal{P} = \emptyset$  ▷ Output set
7:  $\mathcal{F} = \emptyset$  ▷ Fingerprint set
8: EXPLORATIVEDERIVE( $\mathcal{E}_0$ )
9: function EXPLORATIVEDERIVE( $\mathcal{E}$ )
10:   let  $Q$  be a queue storing expressions and depths
11:    $Q.queue([\mathcal{E}_0, 0])$ 
12:   while  $Q$  is not empty do
13:      $[\mathcal{E}, depth] = Q.dequeue()$ 
14:     if  $depth < MaxDepth$  then
15:        $fp = FINGERPRINT(\mathcal{E})$ 
16:       if  $fp \in \mathcal{F}$  then
17:         continue
18:       if  $\mathcal{E}$  is a tensor then
19:          $\mathcal{P} = \mathcal{P} \cup \{\mathcal{E}\}$ 
20:         continue
21:        $\mathcal{F} = \mathcal{F} \cup \{fp\}$ 
22:       for  $r \in \mathcal{R}$  do ▷ Select and apply a rule
23:          $Q.queue([r(\mathcal{E}), depth + 1])$ 
24:       for  $\mathcal{T} \in \mathcal{O}$  do
25:         GUIDEDDERIVE( $\mathcal{E}, \mathcal{T}$ )
26:
27: function GUIDEDDERIVE( $\mathcal{E}, \mathcal{T}$ )
28:   if  $\mathcal{E}$  is a tensor then
29:      $\mathcal{P} = \mathcal{P} \cup \{\mathcal{E}\}$ 
30:     return
31:   for  $r \in \text{SELECTRULES}(\mathcal{E}, \mathcal{T})$  do
32:     GUIDEDDERIVE( $r(\mathcal{E}), \mathcal{T}$ )

```

---

iterator mapping table and the constraints of target operators. For each tensor  $\mathbf{T}$  with index variables  $\vec{x}$ , OLLIE constructs a new tensor,  $\mathbf{T}'$  with index variables  $\vec{x}'$  where  $\mathbf{T}'[\vec{x}'] = \mathbf{T}[\Phi(\vec{x})]$ .

For example, the expression in the inner scope of  $\mathcal{E}_6$  in Figure 6 is mapped to a Matmul operator using the iterator mapping table. By comparing the iterators in the expression and the iterators of a Matmul operator in Table 2, we obtain the following *iterator mapping*:

$$t_1, t_2 \rightarrow m; r, s, f \rightarrow n; c \rightarrow k$$

Thus, to perform this mapping, iterators  $t_1$  and  $t_2$  should be fused to a single variable  $m$ , so do  $r, s$  and  $f$  to  $n$ . After mapping iterators, OLLIE can infer the shape of each tensor from iterator mapping table and construct new tensors from existing tensors. The input tensor  $\mathbf{A}'$  and weight tensor  $\mathbf{K}'$  for Matmul are constructed by the following equation:

$$\mathbf{A}'[m, k] = \mathbf{A}'[t_1 \times W + t_2, c] = \mathbf{A}[t_1, t_2, c] \quad (3)$$



$$\mathbf{K}'[k, n] = \mathbf{K}'[c, r \times S \times F + s \times F + f] = \mathbf{K}[r, s, f, c] \quad (4)$$

, where the mapping functions  $(m, k) = \Phi_A(t_1, t_2, c) = (t_1 \times W + t_2, c)$ ,  $(k, n) = \Phi_K(r, s, f, c) = (c, r \times S \times F + s \times F + f)$ , and  $W$ ,  $S$ , and  $F$  are the range size of iterators  $w$ ,  $s$  and  $f$ . OLLIE automatically generates required tensor layout transformations by instantiating Equation (3) and (4).

### 5.3 Redundancy Pruning

Given an input tensor algebra expression and derivation rules, OLLIE’s optimizer considers all possible combinations of these rules up to a fixed size. However, directly enumerating all possible combinations of rules results in significant redundancy since applying different sequences of derivation rules may reach the same expression. For example, applying the variable substitution rules twice with mapping function  $\Phi$  and  $\Psi$  generates the following expression:

$$\begin{aligned} \mathbf{L}_{\vec{x}} f(\vec{x}) &= \mathbf{L}_{\vec{x}} \{ \mathbf{L}_{\vec{y}} f(\Phi^{-1}(\vec{y})) \} \{ \Phi(\vec{x}) \} \\ &= \mathbf{L}_{\vec{x}} \{ \mathbf{L}_{\vec{y}} \{ \mathbf{L}_{\vec{z}} f(\Phi^{-1}(\Psi^{-1}(\vec{z}))) \} \{ \Psi(\vec{y}) \} \} \{ \Phi(\vec{x}) \} \end{aligned}$$

In the case  $\Psi = \Phi^{-1}$ , the most inner scope in the second line above can be transformed to

$$\mathbf{L}_{\vec{z}} f(\Phi^{-1}(\Psi^{-1}(\vec{z}))) = \mathbf{L}_{\vec{z}} f(\Phi^{-1}(\Phi(\vec{z}))) = \mathbf{L}_{\vec{z}} f(\vec{z})$$

Note that  $\mathbf{L}_{\vec{z}} f(\vec{z})$  is identical to the original expression  $\mathbf{L}_{\vec{x}} f(\vec{x})$ . Therefore, we do not need to apply additional derivation rules on this scope.

OLLIE uses a fingerprint technique to detect redundant scopes. The *fingerprint* is a hash of the expression. It is capable to distinguish the following redundant expressions:

- **Iterator renaming:** iterators should be distinguished by their iterator space, instead of their names, e.g., expressions  $\mathbf{L}_{x=0}^N \mathbf{L}_{y=0}^M f(x, y)$  and  $\mathbf{L}_{y=0}^N \mathbf{L}_{z=0}^M f(y, z)$  are equivalent, and  $(x, y)$  in the former one should be mapped to  $(y, z)$  in the latter one.
- **Summation reordering:** summations can be reordered, e.g.,  $\sum_{\vec{x}} \sum_{\vec{y}} f(\vec{x}, \vec{y})$  is equivalent with  $\sum_{\vec{y}} \sum_{\vec{x}} f(\vec{x}, \vec{y})$ . Note that traversal reordering is not equivalent transformation since it indicates layout transformation.
- **Operands reordering:** operands of commutative binary operations can be reordered, e.g.,  $\mathbf{L}_{\vec{x}} (\mathbf{T}_1[\vec{x}] + \mathbf{T}_2[\vec{x}])$  equals to  $\mathbf{L}_{\vec{x}} (\mathbf{T}_2[\vec{x}] + \mathbf{T}_1[\vec{x}])$ . Operands reordering should be applied for both iterator computation and tensor computation.
- **Tensor renaming:** tensors introduced by different scopes may has the same value.

To satisfy the above features, OLLIE adopts the following design. For a traversal iterator, we use its iterator space and its order relative to all the traversal notations in the current scope as its fingerprint. The order that appeared in the fingerprint

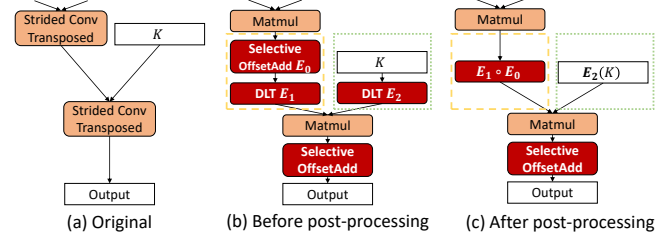


Figure 9: Detailed post-processing for InfoGAN. Red blocks represent eOperators. DLT means data layout transformation.

differentiates traversal iterators with the same iterator spaces but the different locations in the traversal notations. While for summation iterator, we only use its iterator space as its fingerprint. Thus expressions under summation reordering have the same fingerprint. To satisfy operands reordering, we use the operation name and commutative hash for commutative operations, such as addition and non-commutative hash for other operators. The fingerprint of tensors depends on their source. For input tensors, OLLIE calculates the fingerprint by hashing the tensor name. For tensors generated by scopes, their fingerprints are defined by the expressions which generate them.

### 5.4 Post-Processing

**eOperator fusion** OLLIE generates eOperators to facilitate performant transformations. However, although eOperators contain relatively small computation, too many eOperators impact performance as well. To reduce this overhead, OLLIE fuses consecutive eOperators using inter-expression derivations. For example, Figure 9 shows how OLLIE optimizes the InfoGAN model. In the dashed box of Figure 9(b), two eOperators are generated and fused into one kernel by the expression fusion rule.

**Identity eOperator elimination** eOperators produced in derivation can generate identical outputs with inputs, which is called an identity eOperator. For example, although Equation (3) transforms the tensor data layout, but the underlying data remains the same and can be eliminated. To identify identity eOperators, OLLIE squashes input and output tensors to one-dimensional tensor and checks whether the expression is an identical mapping from input to output.

**Compile-time expression evaluation** For expressions only taking weights as input tensors, OLLIE computes them at compile time. For example, in the dotted box of Figure 9, data layout transformation  $E_2$  on weight  $K$  is computed during post postprocess optimization instead of runtime.

## 6 Evaluation

### 6.1 Experimental Setup

**Platform** We evaluate OLLIE on a server with dual Intel Xeon CPU E5-2680 v4 CPUs, an A100 40GB PCIe GPU, and

a V100 32GB PCIe GPU. All experiments use CUDA 11.0.2, cuBLAS 11.1.0, and cuDNN 8.0.3.

**Workloads** We evaluate OLLIE on seven deep learning models, which span various fields and cover both classic models such as ResNet-18 and emerging language models like LongFormer. InfoGAN [12] is a popular generative adversarial network learning disentangled representations from objects. DCGAN [32] leverages deep convolution structures to get hierarchical representations. SRCNN [15] is the first convolutional neural network for image super-resolution. GCN [30] is an image semantic segmentation model named global convolutional network. ResNet-18 [20] is a famous image classification network. CSRNet [27] adopts dilated convolution for congested scene analysis. LongFormer [8] is an improved Transformer architecture network dealing with long-sequence language processing with dilated attention.

## 6.2 End-to-End Performance

We first compare the end-to-end inference time of OLLIE with popular DNN frameworks, including TensorFlow [5] 2.4, TensorFlow XLA [2], TensorRT [35] 8.2, and PET [38]. All frameworks use the same version cuBLAS and cuDNN libraries as backend to fairly show the improvement from OLLIE. For OLLIE, we set the maximum searching depth to 7. For the Longformer case, we implement the new attention operator G2BMM by einsum in TensorFlow and provide an auto-tuned kernel for TensorRT, PET, and OLLIE, since it is not included in the cuBLAS and cuDNN libraries. Figure 10 and Figure 11 shows the end-to-end execution time on A100 and V100 respectively. Detailed operator performance analysis will be shown in §6.4.

OLLIE achieves speedups up to  $2.73\times$  on A100 and  $2.68\times$  on V100. For classical model ResNet-18, OLLIE still achieves speedups up to  $1.33\times$ . OLLIE discovers new optimizations which cannot be found by previous frameworks, such as transforming convolution to Matmul and OffsetAdd (Figure 3b). PET finds many effective optimization and outperforms TensorRT on SRCNN, GCN, and CSRNet. However, OLLIE still achieves speedups over PET since more performant transformations for the same subprograms are discovered. For CSRNet, one of the typical optimizing cases of PET, OLLIE transforms the dilated convolution into non-dilated convolution by expression derivation. This optimization is similar to PET, indicating that OLLIE can contain the optimizations in PET, and discovers further optimizations. We will discuss typical optimizations in §6.3.

## 6.3 Optimization Analysis

To find how OLLIE optimizes models, we illustrate typical optimizations discovered by OLLIE and conduct performance analysis. Their configurations are shown in Table 3.

Table 3: Performance studies on the operators in §6.3. IGEMM, FFT, and WINO in the Algo column refer to implicit GEMM, Fast Fourier Transform, and Winograd convolution algorithms, respectively. The DRAM and L2 columns show the amount of memory access. The input shapes for the following operators are [1, 512, 7, 7], [16, 256, 2, 2], [16, 32, 224, 224] and [8, 10000, 64], respectively. The first three cases are based on cuDNN and cuBLAS, and the last one case uses kernel generated from Ansor.

		Algo	Time (ms)	DRAM (MB)	L2 (MB)
Conv3x3 Figure 3b	Original	WINO	0.126	56.7	70.6
	Optimized	N/A	0.046	10.5	27.5
ConvTranspose Figure 12	Original	IGEMM	0.136	7.74	122
	Optimized	N/A	0.032	8.07	27.8
Conv5x5	Original	FFT	0.854	547	579
	Optimized	WINO	0.528	368	499
G2BMM	Original	N/A	20.3	129	52690
	Optimized	N/A	2.59	41.1	1400

For the Conv3x3 in ResNet-18, OLLIE transforms it to Matmul and an eOperator OffsetAdd according to Figure 3b. OffsetAdd will be fused with following element-wise operators. The profiling data in Table 3 shows that less read and write are required and OLLIE achieves a  $3.65\times$  speedup against cuDNN which selects Winograd algorithm.

OLLIE transforms the ConvTranspose in InfoGAN to Matmul and an eOperator. As shown in Figure 12, OLLIE directly applies Matmul to the kernel and input tensor without padding. Since the ConvTranspose is strided, its input tensor is padded among adjacent elements. For one output element, only part of the outputs of Matmul are required to be summed up. OLLIE automatically performs transformation and produces a selective addition on the outputs of Matmul by expression derivation. In this transformation, a direct computation of GEMM can avoid the redundant computation on ConvTranspose and significantly reduce the L2 access which makes the main contribution of the performance optimization.

## 6.4 Collaboration with Different Backends

Since OLLIE searches expression space, it can cooperate with different backends, including math libraries and schedule-based code generation frameworks. To show the improvements of OLLIE on these backends, we evaluate OLLIE with cuBLAS/cuDNN and TVM [10] with its auto-scheduler Ansor [11]. The evaluation is carried out on the same transformations illustrated in §6.3.

Figure 13 shows OLLIE is beneficial for different backends. For Conv3x3 in ResNet-18 and ConvTranspose in InfoGAN, transforming it to Matmul and an eOperator has significant speedup over both cuDNN and Ansor. The transformation from Conv5x5 to Conv3x3 in SRCNN is beneficial for cuDNN. Such transformation do not have performance improvement on Ansor since Ansor directly tunes original computation, and it cannot adopt efficient algorithms such as

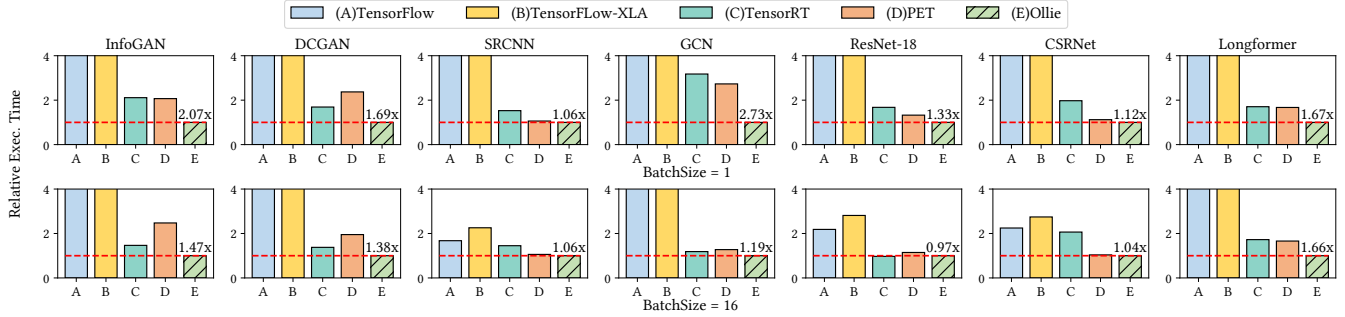


Figure 10: End to end performance on A100 with batch size 1 and 16.

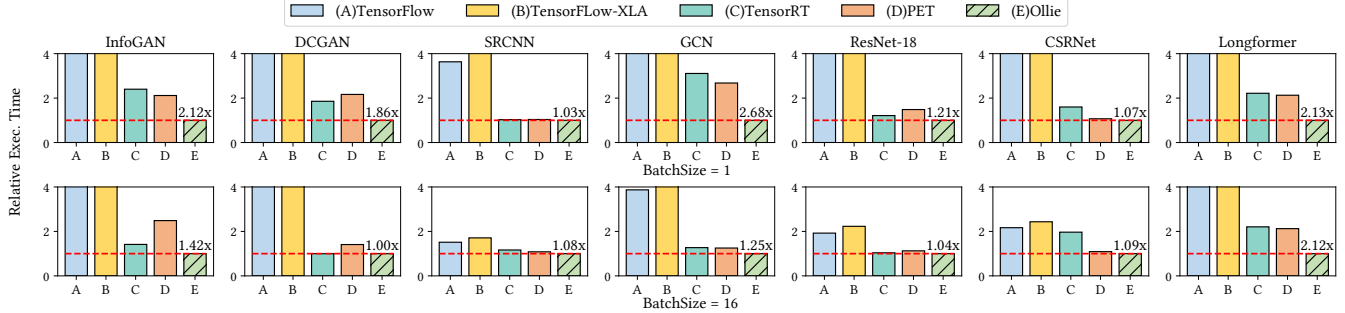


Figure 11: End to end performance on V100 with batch size 1 and 16.

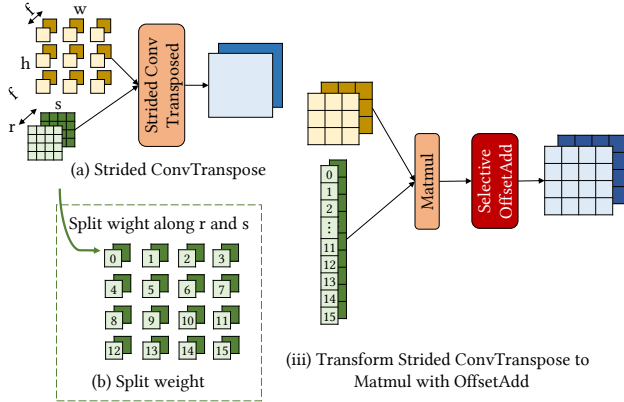


Figure 12: Strided ConvTransposed to Matmul in InfoGAN

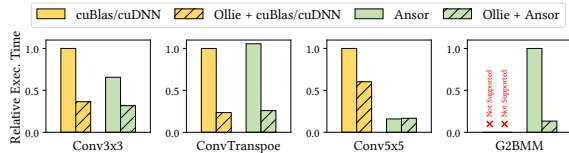


Figure 13: Operator performance before and after optimization (opt) on the math libraries and code generation framework Anso. The input settings are shown in Table 3.

Winograd [26] which is preferred for Conv3x3. For G2BMM operator in Longformer, which is not a pre-defined operator in math libraries, OLLIE is able to transform it from a dilated form to non-dilated form, which brings a speedup of 7.49x since less non-contiguous memory access happens.

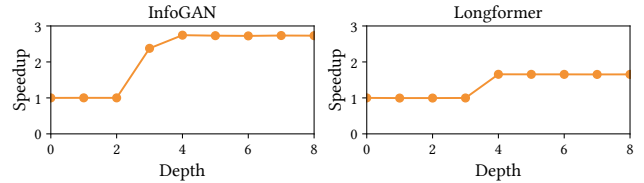


Figure 14: Speedup under different maximum search depths

## 6.5 Analysis on Automated Derivation

The search space of OLLIE is determined by several heuristic parameters, such as the maximum searching depth in the automated derivation algorithm (Algorithm 2). The maximum depth specifies the largest steps of derivation applied to an expression. A larger searching depth enables more potential optimizations but larger searching overhead. In Figure 14, we analyze the speedup OLLIE can achieve with different maximum searching depth in InfoGAN and Longformer. On InfoGAN, OLLIE has improvement when searching step increases from 2 to 4, as new transformations are explored with a deeper search. While for Longformer, the major performance speedup comes from the transformation found in a 4-step derivation. In conclusion, the key takeaway is that OLLIE can achieve most of the performance improvement at moderate depth.

To evaluate the proposed techniques for derivation, we evaluate the searching process on the four cases in Table 3 with and without guided derivation and expression fingerprint. **Hybrid derivation (§5.2)** provides a deterministic derivation direction to avoid enormous search overhead. As shown in Figure 15(a), the search time grows exponentially with the maximum depth of explorative derivation (i.e., *MaxDepth*

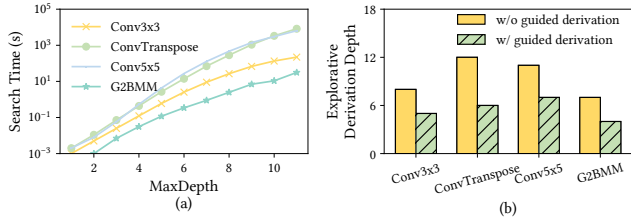


Figure 15: (a) Search time with different  $MaxDepth$ . (b) The number of explorative derivation steps with and without guided derivation.

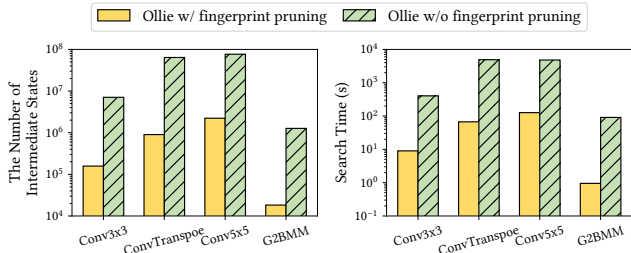


Figure 16: Ablation study of expression fingerprint pruning in Algorithm 2). OLLIE adopts guided derivation to replace explorative derivation. Figure 15(b) shows the number of applied explorative and guided derivations in these cases.

In the case of ConvTranspose, the explorative derivation requires a search with  $MaxDepth = 12$  to discover the target expression. But with guided derivation, OLLIE only requires a search with  $MaxDepth = 6$ , which means that matching a vendor-provided operator needs a 6-step ( $12 - 6$ ) searching and guided derivation can reduce this unnecessary searching. Thus, this optimization leads to a significant reduction of the searching time by more than 99.0%.

**Expression fingerprint (§5.3)** prunes redundant searching states. Figure 16 shows the intermediate states and searching time with and without the fingerprint mechanism. During the enumerating derivation, fingerprint effectively prunes 98.0% of intermediate states by recognizing and reducing duplicate expressions and reduces 98.2% of searching time on average.

With the guided derivation and expression fingerprint, OLLIE finishes searching within two minutes for most subprograms. The searching time of OLLIE is therefore on par with other search-based DNN optimization frameworks, such as TASO, PET, and Anso. OLLIE is able to be deployed in real production environment since the searching cost is one-off for a model and brings persistent benefits.

## 7 Related Work

**Rule-Based Approaches.** Rule-based optimizations are widely used in different tensor programming frameworks. Based on TensorFlow [4], Grappler [1] performs rule-based optimizations like constant folding and layout optimization. TensorFlow XLA [2], TensorRT [35], and DNNFusion [29] similarly perform neural network optimizations. Although rule-based optimizations can efficiently optimize computation

graphs, summarizing and implementing such rules require a large amount of human efforts and expertise.

**Superoptimization-Based Approaches.** TASO [22] and PET [38] try to save human effort in DNN optimization by searching optimized transformations given a set of operators. TASO adopts formal verification techniques to assure the equivalence of transformations. PET further introduces inequivalent transformations and correction mechanism to find more optimizations. Compared with these frameworks, OLLIE extends the search space from POR expressions to general expressions by tensor algebra expression derivation.

**Schedule-Based Optimizations.** Halide [34] decouples a program into computation and schedule and performs schedule space transformations. This idea is widely adopted by many tensor optimization frameworks including TVM [10], FlexTensor [41], and Anso [40]. Orthogonal to schedule-based optimizers, OLLIE focuses on expression space and designs the corresponding expression derivation rules, such as operator matching, to facilitate these new transformations.

## 8 Conclusion

We propose OLLIE, the first derivation-based tensor program framework that enables expression-level optimizations, which extends the search space of tensor programs from predefined operator representable expressions to general expressions. Evaluation results show that OLLIE outperforms state-of-the-art frameworks by up to  $2.73\times$  on NVIDIA A100 and up to  $2.68\times$  on NVIDIA V100.

## References

- [1] Tensorflow graph optimization with grappler; tensorflow core.
- [2] Xla: Optimizing compiler for tensorflow. <https://www.tensorflow.org/xla>, 2017.
- [3] Tensor cores in nvidia volta architecture. <https://www.nvidia.com/en-us/data-center/tensorcore/>, 2018.
- [4] Martín Abadi, Ashish Agarwal, Paul Barham, Eugene Brevdo, Zhifeng Chen, Craig Citro, Greg S. Corrado, Andy Davis, Jeffrey Dean, Matthieu Devin, Sanjay Ghemawat, Ian Goodfellow, Andrew Harp, Geoffrey Irving, Michael Isard, Yangqing Jia, Rafal Jozefowicz, Lukasz Kaiser, Manjunath Kudlur, Josh Levenberg, Dandelion Mané, Rajat Monga, Sherry Moore, Derek Murray, Chris Olah, Mike Schuster, Jonathon Shlens, Benoit Steiner, Ilya Sutskever, Kunal Talwar, Paul Tucker, Vincent Vanhoucke, Vijay Vasudevan, Fernanda Viégas, Oriol Vinyals, Pete Warden, Martin Wattenberg, Martin Wicke,

- Yuan Yu, and Xiaoqiang Zheng. TensorFlow: Large-scale machine learning on heterogeneous systems, 2015. Software available from tensorflow.org.
- [5] Martín Abadi, Paul Barham, Jianmin Chen, Zhifeng Chen, Andy Davis, Jeffrey Dean, Matthieu Devin, Sanjay Ghemawat, Geoffrey Irving, Michael Isard, et al. Tensorflow: A system for large-scale machine learning. In *12th {USENIX} symposium on operating systems design and implementation ({OSDI} 16)*, pages 265–283, 2016.
- [6] Dario Amodei, Sundaram Ananthanarayanan, Rishita Anubhai, Jingliang Bai, Eric Battenberg, Carl Case, Jared Casper, Bryan Catanzaro, Qiang Cheng, Guoliang Chen, et al. Deep speech 2: End-to-end speech recognition in english and mandarin. In *International conference on machine learning*, pages 173–182. PMLR, 2016.
- [7] Riyadh Baghdadi, Jessica Ray, Malek Ben Romdhane, Emanuele Del Sozzo, Abdurrahman Akkas, Yunming Zhang, Patricia Suriana, Shoaib Kamil, and Saman Amarasinghe. Tiramisu: A polyhedral compiler for expressing fast and portable code. In *2019 IEEE/ACM International Symposium on Code Generation and Optimization (CGO)*, pages 193–205. IEEE, 2019.
- [8] Iz Beltagy, Matthew E Peters, and Arman Cohan. Longformer: The long-document transformer. *arXiv preprint arXiv:2004.05150*, 2020.
- [9] Kumar Chellapilla, Sidd Puri, and Patrice Simard. High performance convolutional neural networks for document processing. In *Tenth international workshop on frontiers in handwriting recognition*. Suvisoft, 2006.
- [10] Tianqi Chen, Thierry Moreau, Ziheng Jiang, Haichen Shen, Eddie Q. Yan, Leyuan Wang, Yuwei Hu, Luis Ceze, Carlos Guestrin, and Arvind Krishnamurthy. TVM: end-to-end optimization stack for deep learning. *CoRR*, abs/1802.04799, 2018.
- [11] Tianqi Chen, Lianmin Zheng, Eddie Yan, Ziheng Jiang, Thierry Moreau, Luis Ceze, Carlos Guestrin, and Arvind Krishnamurthy. Learning to optimize tensor programs. In *Advances in Neural Information Processing Systems 31*, NeurIPS’18. 2018.
- [12] Xi Chen, Yan Duan, Rein Houthoofd, John Schulman, Ilya Sutskever, and Pieter Abbeel. Infogan: Interpretable representation learning by information maximizing generative adversarial nets. In *Proceedings of the 30th International Conference on Neural Information Processing Systems*, pages 2180–2188, 2016.
- [13] Sharan Chetlur, Cliff Woolley, Philippe Vandermersch, Jonathan Cohen, John Tran, Bryan Catanzaro, and Evan Shelhamer. cudnn: Efficient primitives for deep learning. *CoRR*, abs/1410.0759, 2014.
- [14] Dense Linear Algebra on GPUs. <https://developer.nvidia.com/cublas>, 2016.
- [15] Chao Dong, Chen Change Loy, Kaiming He, and Xiaoou Tang. Learning a deep convolutional network for image super-resolution. In *European conference on computer vision*, pages 184–199. Springer, 2014.
- [16] Ross Girshick. Fast r-cnn. In *Proceedings of the IEEE international conference on computer vision*, pages 1440–1448, 2015.
- [17] Sorin Grigorescu, Bogdan Trasnea, Tiberiu Cocias, and Gigel Macesanu. A survey of deep learning techniques for autonomous driving. *Journal of Field Robotics*, 37(3):362–386, 2020.
- [18] Anmol Gulati, James Qin, Chung-Cheng Chiu, Niki Parmar, Yu Zhang, Jiahui Yu, Wei Han, Shibo Wang, Zhengdong Zhang, Yonghui Wu, et al. Conformer: Convolution-augmented transformer for speech recognition. *arXiv preprint arXiv:2005.08100*, 2020.
- [19] Kaiming He, Georgia Gkioxari, Piotr Dollár, and Ross Girshick. Mask r-cnn. In *Proceedings of the IEEE international conference on computer vision*, pages 2961–2969, 2017.
- [20] Kaiming He, Xiangyu Zhang, Shaoqing Ren, and Jian Sun. Deep residual learning for image recognition. In *Proceedings of the IEEE Conference on Computer Vision and Pattern Recognition, CVPR*, 2016.
- [21] Zhihao Jia, Oded Padon, James Thomas, Todd Warszawski, Matei Zaharia, and Alex Aiken. Taso: optimizing deep learning computation with automatic generation of graph substitutions. In *Proceedings of the 27th ACM Symposium on Operating Systems Principles*, pages 47–62, 2019.
- [22] Zhihao Jia, Oded Padon, James J. Thomas, Todd Warszawski, Matei Zaharia, and Alex Aiken. TASSO: optimizing deep learning computation with automatic generation of graph substitutions. In Tim Brecht and Carey Williamson, editors, *Proceedings of the 27th ACM Symposium on Operating Systems Principles, SOSP 2019, Huntsville, ON, Canada, October 27-30, 2019*, pages 47–62. ACM, 2019.
- [23] Norman P Jouppi, Cliff Young, Nishant Patil, David Patterson, Gaurav Agrawal, Raminder Bajwa, Sarah Bates, Suresh Bhatia, Nan Boden, Al Borchers, et al. In-datascenter performance analysis of a tensor processing

- unit. In *Proceedings of the 44th annual international symposium on computer architecture*, pages 1–12, 2017.
- [24] B Ravi Kiran, Ibrahim Sobh, Victor Talpaert, Patrick Mannion, Ahmad A Al Sallab, Senthil Yogamani, and Patrick Pérez. Deep reinforcement learning for autonomous driving: A survey. *IEEE Transactions on Intelligent Transportation Systems*, 2021.
- [25] Johannes Langer. *Band Matrices in Recurrent Neural Networks for Long Memory Tasks*. PhD thesis, 2018.
- [26] Andrew Lavin and Scott Gray. Fast algorithms for convolutional neural networks. In *2016 IEEE Conference on Computer Vision and Pattern Recognition (CVPR)*, pages 4013–4021. IEEE, 2016.
- [27] Yuhong Li, Xiaofan Zhang, and Deming Chen. Csrnet: Dilated convolutional neural networks for understanding the highly congested scenes. In *Proceedings of the IEEE conference on computer vision and pattern recognition*, pages 1091–1100, 2018.
- [28] Liangkai Liu, Sidi Lu, Ren Zhong, Baofu Wu, Yongtao Yao, Qingyang Zhang, and Weisong Shi. Computing systems for autonomous driving: State of the art and challenges. *IEEE Internet of Things Journal*, 8(8):6469–6486, 2020.
- [29] Wei Niu, Jiexiong Guan, Yanzhi Wang, Gagan Agrawal, and Bin Ren. Dnnfusion: accelerating deep neural networks execution with advanced operator fusion. In *Proceedings of the 42nd ACM SIGPLAN International Conference on Programming Language Design and Implementation*, pages 883–898, 2021.
- [30] Chao Peng, Xiangyu Zhang, Gang Yu, Guiming Luo, and Jian Sun. Large kernel matters—improve semantic segmentation by global convolutional network. In *Proceedings of the IEEE conference on computer vision and pattern recognition*, pages 4353–4361, 2017.
- [31] Tensors and Dynamic neural networks in Python with strong GPU acceleration. <https://pytorch.org>, 2017.
- [32] Alec Radford, Luke Metz, and Soumith Chintala. Un-supervised representation learning with deep convolutional generative adversarial networks. *arXiv preprint arXiv:1511.06434*, 2015.
- [33] Jonathan Ragan-Kelley, Connelly Barnes, Andrew Adams, Sylvain Paris, Frédo Durand, and Saman Amarasinghe. Halide: A language and compiler for optimizing parallelism, locality, and recomputation in image processing pipelines. In *Proceedings of the 34th ACM SIGPLAN Conference on Programming Language Design and Implementation*, PLDI ’13, 2013.
- [34] Jonathan Ragan-Kelley, Connelly Barnes, Andrew Adams, Sylvain Paris, Frédo Durand, and Saman P. Amarasinghe. Halide: a language and compiler for optimizing parallelism, locality, and recomputation in image processing pipelines. In Hans-Juergen Boehm and Cormac Flanagan, editors, *ACM SIGPLAN Conference on Programming Language Design and Implementation, PLDI ’13, Seattle, WA, USA, June 16-19, 2013*, pages 519–530. ACM, 2013.
- [35] NVIDIA TensorRT: Programmable inference accelerator. <https://developer.nvidia.com/tensorrt>, 2017.
- [36] Aravind Vasudevan, Andrew Anderson, and David Gregg. Parallel multi channel convolution using general matrix multiplication, 2017.
- [37] Ashish Vaswani, Noam Shazeer, Niki Parmar, Jakob Uszkoreit, Llion Jones, Aidan N Gomez, Łukasz Kaiser, and Illia Polosukhin. Attention is all you need. In *Advances in neural information processing systems*, pages 5998–6008, 2017.
- [38] Haojie Wang, Jidong Zhai, Mingyu Gao, Zixuan Ma, Shizhi Tang, Liyan Zheng, Yuanzhi Li, Kaiyuan Rong, Yuanyong Chen, and Zhihao Jia. Pet: Optimizing tensor programs with partially equivalent transformations and automated corrections. In *15th USENIX Symposium on Operating Systems Design and Implementation (OSDI 21)*, pages 37–54, 2021.
- [39] Yonghui Wu, Mike Schuster, Zhifeng Chen, Quoc V Le, Mohammad Norouzi, Wolfgang Macherey, Maxim Krikun, Yuan Cao, Qin Gao, Klaus Macherey, et al. Google’s neural machine translation system: Bridging the gap between human and machine translation. *arXiv preprint arXiv:1609.08144*, 2016.
- [40] Lianmin Zheng, Chengfan Jia, Minmin Sun, Zhao Wu, Cody Hao Yu, Ameer Haj-Ali, Yida Wang, Jun Yang, Danyang Zhuo, Koushik Sen, et al. Ansor: generating high-performance tensor programs for deep learning. In *14th {USENIX} Symposium on Operating Systems Design and Implementation ({OSDI} 20)*, pages 863–879, 2020.
- [41] Size Zheng, Yun Liang, Shuo Wang, Renze Chen, and Kaiwen Sheng. Flextensor: An automatic schedule exploration and optimization framework for tensor computation on heterogeneous system. In *Proceedings of the Twenty-Fifth International Conference on Architectural Support for Programming Languages and Operating Systems*, pages 859–873, 2020.